[1]Dr. K. Srinivasan,

Mr. TKS. Sathyanarayanan,

Mr. B. Partheeban

Optimal Component Design of a Solar-Fed Modified Z-Source Inverter for Induction Motor Drive Systems

Abstract— This paper examines the performance of an induction motor drive system utilizing a cost-effective induction motor in conjunction with a reduced-switch, three-phase modified Z-source inverter (RSTPZSI). In the proposed approach, a 4-switch, 3-phase modified Z-source inverter replaces the conventional 6-switch, 3-phase inverter (6S3P). By employing this novel inverter configuration, the modified Z-source system delivers improved performance while reducing construction costs. A key feature of the proposed model is the inclusion of a specific LC network in the DC link and a DC link capacitor that replaces the capacitor leg typically found in traditional inverters. This redesigned Z-source inverter is capable of producing output voltages higher than the line voltage. To validate this approach, simulation results were compared with those of the traditional six-switch inverter. The system was implemented in real-time using a PIC16F84A microcontroller on a 0.5 HP motor prototype. Both theoretical analysis and experimental results demonstrate that the modified Z-source inverter reduces line harmonics, improves power factor and reliability, and extends the output voltage range.

Index Terms— z source inverter, four switch three phase inverter, voltage sags.

I. INTRODUCTION

The Modified Z-Source Inverter (ZSI), illustrated in Fig. 1, was designed to address the inherent limitations of conventional voltage source inverters (VSI) and current source inverters (CSI). In traditional voltage source inverters, simultaneous conduction of both switches in the same phase leg is avoided to prevent short circuits. The innovative four-switch, three-phase modified Z-source inverter overcomes this issue by incorporating an impedance network (Z-network) in place of the standard DC link. This Z-source inverter effectively utilizes shoot-through states, allowing both switches in a single leg to operate concurrently, thereby boosting the DC bus voltage. Consequently, the modified Z-source inverter is capable of raising the output voltage beyond the input DC bus voltage. Additionally, the system's enhanced reliability offers improved circuit protection.. This design offers a highly reliable and cost-efficient single-stage solution for buck-boost power conversion. To further reduce costs and enhance voltage levels, the switched-inductor Z-source four-switch inverter provides chopper functionality to effectively address these challenges. The primary function of the switched inductors is to increase voltage and protect the switches during the shoot-through phase. Traditionally, three-phase, six-switch inverters have been commonly used in variable-speed induction motor drives. However, these inverters have several drawbacks, including higher losses due to the use of six switches, complex control algorithms, and the need for intricate gate drive circuits to generate six PWM logic signals. Recently, there has been growing interest in the use of four-switch, three-phase inverters for uninterruptible power supplies and variable-speed drives. The four-switch, three-phase inverter offers several advantages over the conventional six-switch configuration, such as reduced costs due to fewer switches, lower switching losses, fewer gate drive circuits, simplified control algorithms for PWM generation, and decreased risk of switch failure due to reduced interaction between switches. Additionally, when combined with a modified Z-source, the four-switch, three-phase inverter effectively utilizes shoot-through states to increase the DC bus voltage by enabling both switches in the same leg to conduct simultaneously.

[1] Department of Electrical and Electronics Engineering
Tagore Engineering college, Chennai-600127.
omsrivas@yahoo.co.in, tkssujaakil@gmail.com, partheeban.balakrishnan@gmail.com

Currently, two primary inverter configurations are employed in adjustable speed drives: the traditional three-phase PWM inverter and the three-phase PWM inverter combined with a DC-DC boost converter. The conventional PWM inverter subjects both the switching devices and the motor to significant stress, potentially limiting the motor's constant power speed range. In contrast, the PWM inverter paired with a DC-DC boost converter mitigates these stresses and overcomes these limitations. However, this configuration introduces drawbacks such as higher costs and added complexity due to the two-stage power conversion process.

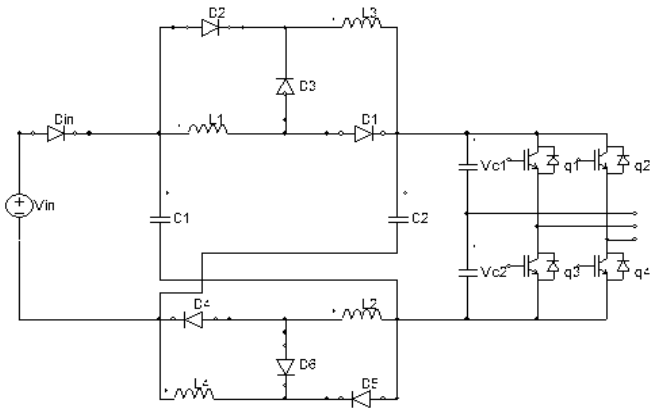

Fig.1 four switch three phase inverter with modified z source inverter

The newly developed four-switch, three-phase modified Z-Source Inverter for induction motor (IM) drives offers a significant advantage by enhancing output voltage through the utilization of a shoot-through state, a feature absent in conventional voltage source inverters. This innovative inverter design delivers a cost-effective, streamlined, single-stage solution for induction motor drive applications.

II.DRIVE SYSTEM MODELLING

The block diagram of the proposed system is illustrated in Fig. 2. The drive system includes a solar panel, a modified Z-source network, a three-phase four-switch inverter, a three-phase induction motor, and control circuits. The direct current (DC) supply is sourced from the solar panel and directed to the inverter, where a sinusoidal pulse width modulation (PWM) generator produces the required pulses. The inverter switches function based on a predetermined switching pattern, and the output from the four-switch inverter is supplied to the three-phase induction motor.

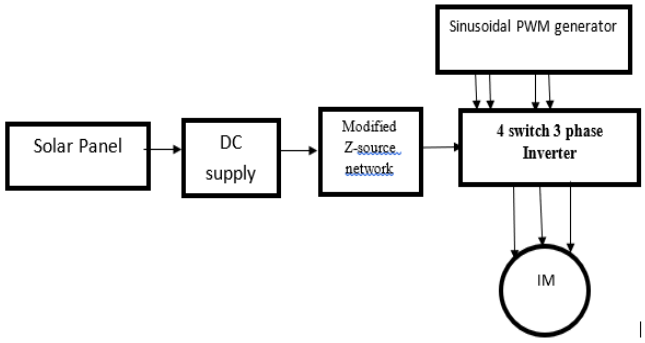

Fig .2.The block diagram of the proposed system

The detailed modeling of the drive system encompasses the inverter, induction motor, and Z-source inverter, which will be further elaborated upon in the subsequent subsections.

A. MODELLING OF PHOTOVOLTAIC ARRAYS

Photovoltaics refers to the process of converting light directly into electrical energy. Certain materials exhibit a property called the photoelectric effect, enabling them to absorb light photons and emit electrons. Each solar cell generates a modest amount of power, typically ranging from 1 to 2 watts. To increase the overall power output, these cells are assembled into a sealed unit referred to as a solar module. The fundamental equation derived from semiconductor theory provides a mathematical representation of the current-voltage (I-V) characteristics of an ideal photovoltaic cell.

$$I=Iph -Ir(exp[\frac{q(V+IR_S}{akT}]-1) - \frac{V+IR_S}{R_p} \quad (1)$$

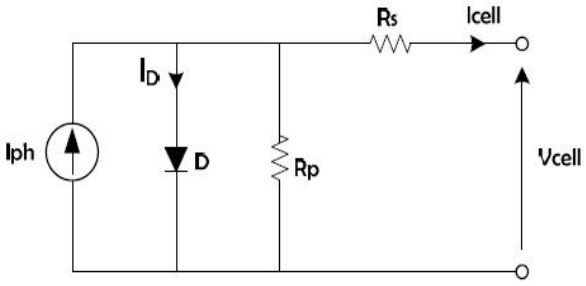

Fig3. PV Equivalent Circuit

The current generated by incident light, referred to as ***I***ph, is directly proportional to solar irradiation. The reverse saturation or leakage current of the diode, denoted as ***Ir***, is influenced by the temperature of the p-n junction. The diode ideality factor is represented by "a," while "q" signifies the electron charge, which is measured at [1.60217646 × 10^{-19} C]. Additionally, "k" denotes the Boltzmann constant, valued at [1.3806503 × 10^{-23} J/K]. The equivalent circuit of a photovoltaic (PV) cell is illustrated in Fig. 3. A single PV cell is characterized by a rated voltage of 0.51 V and a rated power output of 0.3 W. In practical applications, photovoltaic arrays are composed of multiple interconnected cells. When an array consists of Np parallel cell connections, the photovoltaic and saturation currents can be represented accordingly.

$$I_{pv}=I_{pv,n}+KI\Delta T(\frac{G}{G_n}) \quad (2)$$

The light-generated current under standard conditions, usually defined at 25°C and 1000 W/m², is denoted as ***I***pv,n. The variable T is defined as the difference between the actual temperature (T) and the nominal temperature (Tn) measured in Kelvin. The irradiation on the surface of the device is indicated as G [W/m²], while Gn represents the nominal irradiation level.

B. FOUR SWITCH THREE PHASE INVERTER MODEL

In this analysis, the inverter switches are treated as ideal power switches, labeled as q1, q2, q3, and q4. The circuit configuration includes four switches and four diodes, which are employed to produce two line-to-line voltages, V13 and V23. The voltage V12 is derived from a split-capacitor bank within the DC link, in accordance with Kirchhoff's voltage law. Based on the circuit's design, the maximum peak value of the line-to-line voltage can attain Vdc/2.

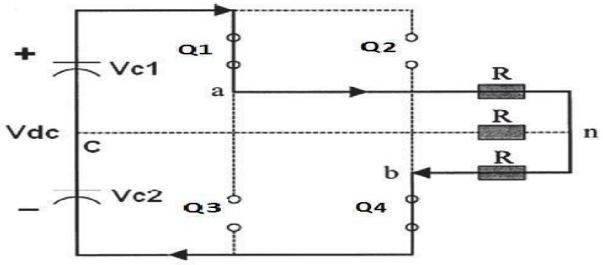

Fig.4. Inverter switching state (0,0)

The conduction states of the power switches are represented by binary variables q1 to q4. In this context, a binary value of "1" denotes a closed switch, while a value of "0" indicates an open switch. The pairs q1-q3 and q2-q4 are complementary, resulting in the equations q3 = 1 - q1 and q4 = 1 - q2. It is assumed that a stable voltage is maintained across the two dc-link capacitors, with Vc1 = Vc2 = Vdc/2, where Vdc represents a constant dc-link voltage. The pole voltages V1, V2, and V3 are determined by the states of the power switches and are expressed in terms of the binary variables q1 and q2, as well as the dc-link voltage.

$$V_1 = (2q_1 - 1)\, V_{dc}/2 \quad (3)$$

$$V_2 = (2q_2 - 1)\, V_{dc}/2 \quad (4)$$

$$V_3 = 0 \quad (5)$$

In a configuration with four switches, there are four distinct switching states: (0, 0), (0, 1), (1, 0), and (1, 1). In the case of a six-switch converter, the states (0, 0) and (1, 1) are classified as zero-vectors. When the motor load is substituted with a resistive load, these zero-vectors fail to supply the necessary dc-link voltage to the load, resulting in no current flow. Conversely, in the four-switch converter, one phase of the motor is continuously connected to the midpoint of the dc-link capacitors, allowing current to flow even during the zero-vector states, as shown in Fig. 4. Moreover, for the states (0, 1) and (1, 0), the phase linked to the midpoint of the dc-link capacitors is uncontrolled, with only the current from the other two phases passing through this phase. If the load is ideally balanced and the capacitor voltages are equal, there will be no current in the uncontrolled phase during the (0, 1) and (1, 0) states. Significant oscillations in the voltage across the two dc-link capacitors, resulting from the current circulating through the capacitive bank of one phase, can lead to considerable ripples, distortions, and imbalances in the output currents of the inverter. The switching states (1, 1) and (0, 0) contribute to an unbalanced load on the split dc-link capacitors, causing one half of the link to discharge more rapidly than the other and ultimately creating a voltage imbalance.

The potential values for the pole voltages V1 and V2 are determined by the states of the switches q1 and q2. To elucidate the operating modes, the induction motor load is replaced with a resistive load, leading to four switching states characterized by particular pole voltages.

$$V_1 = V_2 = -\frac{V_{dc}}{2}, \text{ when } q_1 = q2 = 0 \;;$$

$$V_1 = \frac{V_{dc}}{2}, V_2 = -\frac{V_{dc}}{2}; \text{ when } q1=1, q2 = 0 \;;$$

$$V_1 = -\frac{V_{dc}}{2}, V_2 = \frac{V_{dc}}{2} \text{when } q1 = 0, q2 = 1$$

$$V_1 = V2 = \frac{V_{dc}}{2}, \text{ when } q1 = q2 = 1$$

The phase to neutral voltage can be defined as

$$V_{01}= V_1- V_{n0} \quad (6)$$

$$V_{02}= V2 - V_{n0} \quad (7)$$

$$V_{03}= V_3- V_{n0} \quad \text{and } V_3= 0 \quad (8)$$

where "n" is the centre point of split capacitors, "o" is the neutral point of IM windings and V_{no} is the voltage between the centre point of split capacitors and the neutral point of IM windings.

Normally the induction motor load phase voltage are balanced

$$V_{an}+V_{bn}+V_{cn} = 0$$

$$V_{n0}=\frac{V_{dc}}{6}(2q1+2q2-2) \quad (9)$$

Table 1 Switching function and output voltages from inverter

Switching Function		Switch ON		Output voltage		
q1	q2	T_1 =q1	T_3=q2	V_{01}	V_{02}	V_{03}
0	0	T_2	T_4	$-\frac{V_{dc}}{6}$	$-\frac{V_{dc}}{6}$	$\frac{V_{dc}}{3}$
0	1	T_2	T_3	$-\frac{V_{dc}}{2}$	$\frac{V_{dc}}{2}$	0
1	0	T_1	T_4	$\frac{V_{dc}}{2}$	$-\frac{V_{dc}}{2}$	0
1	1	T_1	T_3	$\frac{V_{dc}}{6}$	$\frac{V_{dc}}{6}$	$-\frac{V_{dc}}{3}$

For better realization, the three phase quantities are transformed to αβ quantities.

The phase to neutral voltage can be derived as follows

Substituting Equations (7) and (1) in (4)

$$V_{01}= (\frac{V_{dc}}{6}) (4q_1-2q_2-1) \quad (10)$$

$$V_{02}= (\frac{V_{dc}}{6}) (4q_2-2q_1-1) \quad (11)$$

$$V_{03}= (\frac{V_{dc}}{6}) (-2q_1-2q_2+2) \quad (12)$$

$$v\alpha\beta = K\ v123 \quad (13)$$

$$K= \sqrt{\frac{2}{3}}\begin{bmatrix} 1 & -\frac{1}{2} & -\frac{1}{2} \\ 0 & \sqrt{\frac{3}{2}} & -\sqrt{\frac{3}{2}} \end{bmatrix} \quad (14)$$

Where $v\alpha\beta = [\ v\alpha, v\beta]^T$, $v123 = [\ v01\ v02\ v03]^T$

The induction motor is assumed to be symmetric with its neutral wire disconnected. The voltage components are given by

$$v\alpha = \sqrt{\frac{2}{3}}\,(q_1 V_{dc} - (\frac{q_2}{2})V_{dc} - (\frac{V_{dc}}{4})) \quad (15)$$

$$v\beta = \sqrt{\frac{2}{3}}\,(\,(\sqrt{\frac{3}{2}})q_2 V_{dc} - (\sqrt{\frac{3}{4}})\,V_{dc}) \quad (16)$$

Table 2

The combinations of switch states

Q1	Q2	V= $v\alpha$+j$v\beta$
0	0	V1= $(\frac{V_{dc}}{\sqrt{6}})e^{-j2\pi/3}$
1	0	V1= $(\frac{V_{dc}}{\sqrt{6}})e^{-j2\pi/3}$
1	1	V1= $(\frac{V_{dc}}{\sqrt{6}})e^{-j2\pi/3}$
0	1	V1= $(\frac{V_{dc}}{\sqrt{6}})e^{-j2\pi/3}$

C. MODIFIED Z SOURCE MODEL

The modified Z-source inverter addresses the limitations of conventional source inverters. This advanced inverter integrates a distinctive impedance network with both the main inverter circuit and the power supply. It exhibits several unique characteristics when compared to traditional voltage source inverters and current source inverters. The impedance network utilizes a four-switch three-phase inverter paired with an induction motor load. A rectifier converts the alternating current (AC) voltage into direct current (DC) voltage, which is then routed to the impedance network, consisting of four identical inductors (L1, L2, L3, L4) and two identical capacitors (C1, C2). The inductors are arranged in series arms, while the capacitors are positioned in diagonal arms. This modified Z-network can either step up or step down the input voltage based on the specified boosting factor. Additionally, it functions as a second-order filter. The main circuits of the inverter include four switches, with gating signals generated via Discontinuous Pulse Width Modulation. It is assumed that the inductors (L1, L2, L3, and L4) and capacitors (C1 and C2) possess equal inductance and capacitance values.Fig.5.Equivalent circuit of the impedance source inverter

III. RESULT AND DISCUSSIONS

The proposed system has been evaluated, and the performance of the inverter configuration along with its control strategy has been validated using Matlab software. The current and voltage waveforms of the four-switch three-phase modified Z-source inverter exhibit patterns similar to those of the conventional six-switch three-phase inverter under

identical conditions. The initial phase current remains within acceptable limits. The steady-state waveform of the three-phase current, as illustrated in Figure 8, demonstrates nearly balanced conditions for both the Four-Switch Three-Phase Inverter (FSTPI) and the Six-Switch Three-Phase Inverter (SSTPI).

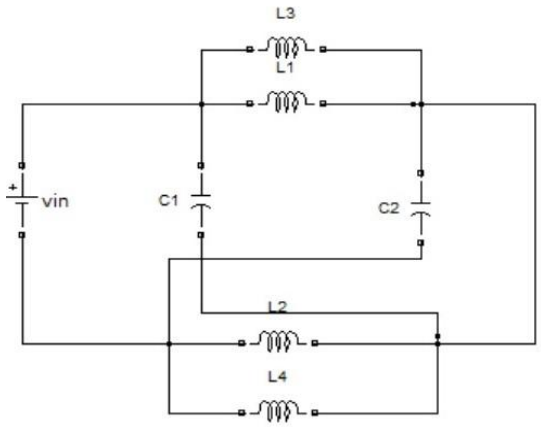

Fig.5.Equivalent circuit of the impedance source inverter

Figure 6.4 illustrates the Simulink model of the modified Z-source inverter. The diagram indicates that the DC supply is sourced from the solar panel and fed into the inverter, which converts the DC supply to an AC supply for the motor. The inverter switches operate on and off according to the duty cycle. By utilizing the scope, the waveforms for stator current, rotor current, electromagnetic torque, and speed can be analyzed.

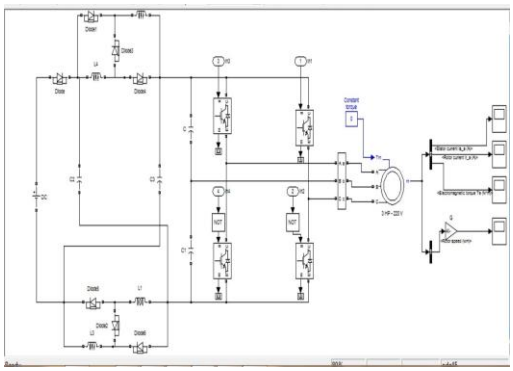

Fig 6 Simulink Diagram of Modified Z Source Inverter

The effectiveness of the Z-Source Inverters is demonstrated by the absence of overshoot, undershoot, and zero steady-state error in the speed response. Figures 8 and 9 illustrate that the speed response and harmonic distortion of the FSTP-Z-Source inverter-based induction motor drive are comparable to those of the conventional Pulse Width Modulation (PWM) inverter-based drive, as shown in Figures 12 and 13. The Total Harmonic Distortion (THD) for the FSTP-Z-Source inverter is measured at 4.29%, while the THD for the six-switch three-phase PWM inverter is recorded at 6.61%, as presented in Figure 12. These results indicate that the performance of the four-switch three-phase inverter-based drive closely aligns with that of the traditional six-switch three-phase inverter. The analysis and simulation results suggest that this inverter can significantly simplify control algorithms and reduce costs.

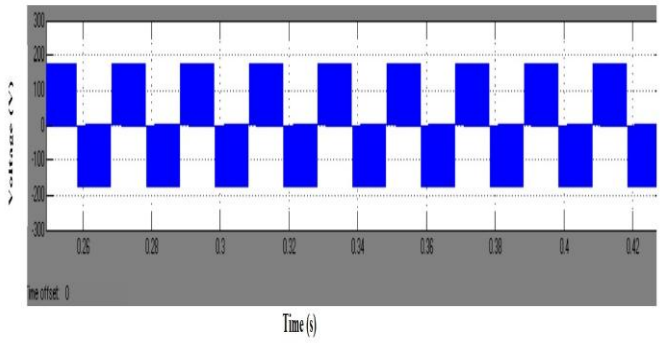

.

Fig.7 FSTP modified Z-source voltage waveform

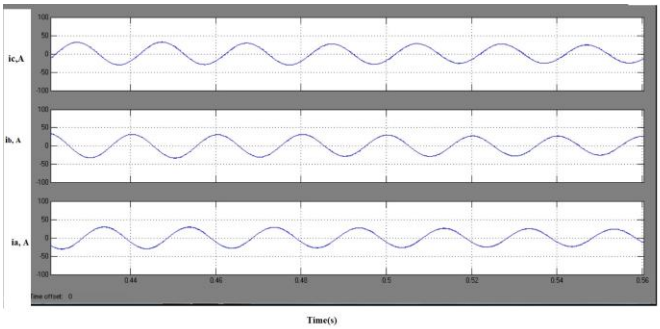

Fig.8 FSTP modified Z-source inverter stator currents

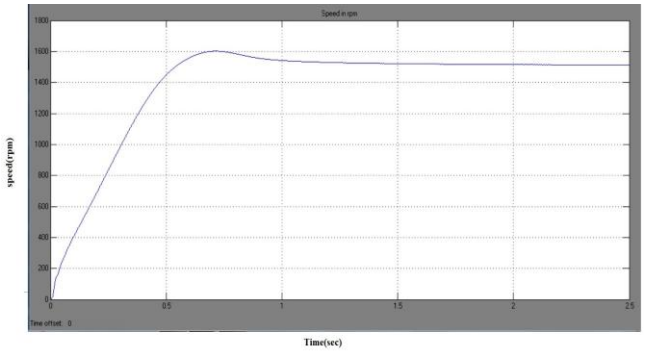

Fig.9 FSTP modified Z-source inverter speed response

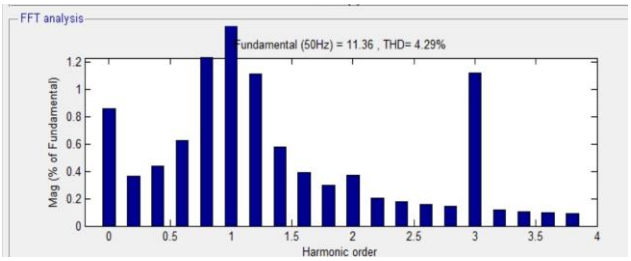

Fig.10 FSTP modified Z-source inverter harmonic spectrum

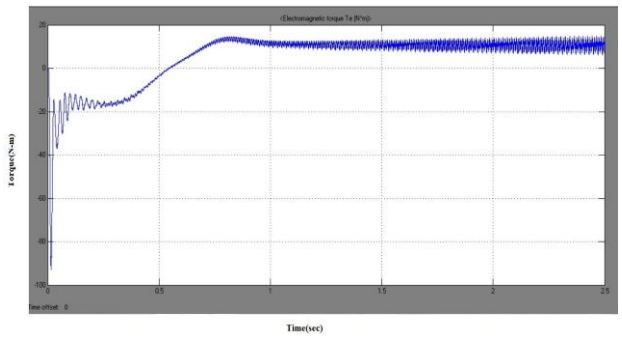

Fig.11 FSTP modified Z-source inverter electromagnetic torque

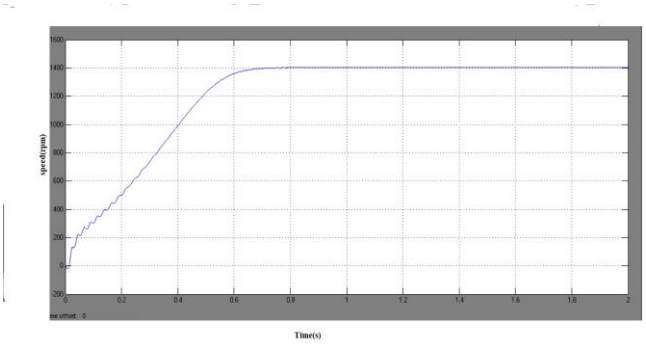

Fig .12.Speed response of conventional inverter fed induction motor drive

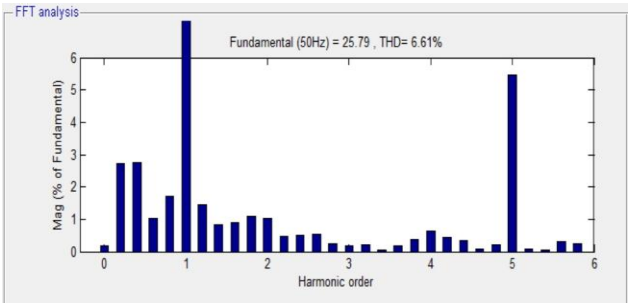

Fig.13.harmonic spectrum of conventional inverter fed Induction Motor Drive

IV. EXPERIMENTAL RESULTS

A laboratory prototype has been developed to validate the operation of the system. The pulse width modulation (PWM) control of the modified Z-source inverter, specifically the FSTP variant, was evaluated using a PIC 16F84A microcontroller in conjunction with a three-phase induction motor. The experimental setup employed a three-phase induction motor with a wound rotor, rated at 0.5 horsepower, as the load. The experimental waveforms are depicted in Figure 15. The direct current (DC) voltage across the inverter bridge was boosted by a factor of 1.21. Furthermore, it is evident that the line current exhibits significantly fewer harmonics compared to conventional adjustable speed drives (ASDs).

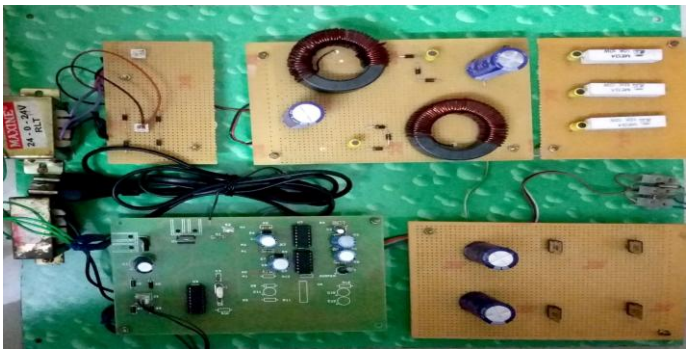

Fig 14 hardware circuit

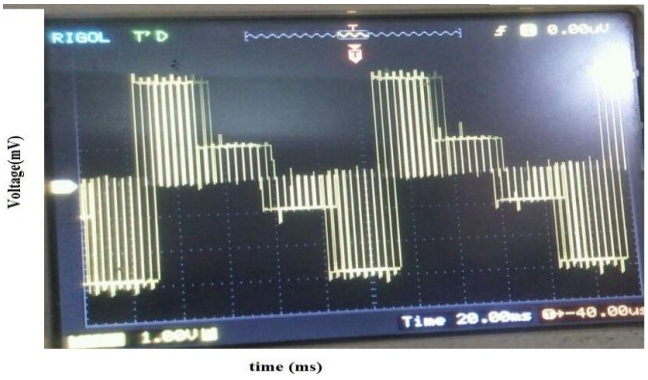

Fig 15 .output of the modified z source

V.CONCLUSION

This research presents a modified Z-source inverter design with a simplified switch configuration, addressing the limitations of traditional inverters. The enhanced Z-source inverter shows improved efficiency, increased reliability, and a more cost-effective power conversion system. Performance indicators for a three-phase induction motor, including stator current, rotor current, rotor speed, and electromagnetic torque, have been evaluated through simulations, highlighting its beneficial characteristics. The modified Z-source inverter features a unique impedance network that connects the inverter's primary circuit to the power source, offering distinct operational advantages. It can increase the input voltage without the need for a chopper circuit, thus enhancing efficiency, lowering costs, and reducing the number of required gate components. Additionally, the switching stress is significantly minimized.

REFERENCES

[1]. Zhang, Z., Li, Y., & Chen, J.”A Review of Four-Switch Three-Phase Inverters for Renewable Energy Applications.” Renewable and Sustainable Energy Reviews, 2021; 120: 109578.
[2]. El-Zonkoly, M. A. E. O., & El-Sayed, K. M. “Performance Evaluation of Four-Switch Three-Phase Inverters in Electric Vehicle Applications.” IEEE Transactions on Industrial Electronics
2020; 66, 1155-1164.
[3]. Kumar, P. R., Reddy, A. P. R., & Prasad, D. B.”Applications of Four-Switch Inverters in Industrial Motor Drives: A Comparative Analysis.” Journal of Electrical Engineering & Technology, 2022; 14: 1941-1952
[4]. Rajasekaran, S. G. T., Rao, R. K., & Kumar, V. K.” Integration of Four-Switch Three-Phase Inverters in Solar Photovoltaic Systems.” Energy Reports, 2019; 6: 256-265

[5]. Rodriguez, J. M., Figueroa, A. J. F., & Gonzalez, E. L." Fault-Tolerant Control of Four-Switch Three-Phase Inverters in Renewable Energy Systems" IEEE Access, 2023; 8: 1214-1223.
[6]. Zhang, H., Smith, M. P. T. S., & Wu, Q.**"** Enhanced Modulation Techniques for Four-Switch Inverters in HVAC Applications",Energy Conversion and Management, 2020: 178; 157-166.
[7]. Gupta, R. B., Shams, S. H., & Rahman, F. M." Evaluating the Performance of Four-Switch Inverters in Wind Energy Conversion Systems."nternational Journal of Renewable Energy Research, 2021: 11; 65-74.
[8]. Thangavel, A. C. J., Manickavasagam, L. J., & Vijayan, T. S. G."Application of Four-Switch Inverters in Electric Vehicle Traction Drives."Journal of Power Electronics, 2022;18: 88-99.

[9] Niaboli Guilani M, Ardeshir G. A mathematical method to realize complex poles in a high-order passive switchedcapacitor filter. International Journal of Circuit Theory and Applications 2019; 47 (11): 1762-1774.

[10] Forouzesh M, Siwakoti YP, Gorji SA, Blaabjerg F, Lehman B. Step-up dc–dc converters: a comprehensive review of voltage-boosting techniques, topologies, and applications. IEEE Transactions on Power Electronics 2017; 32 (12): 9143-9178.

[11] Sandeep N, Ali JSM, Yaragatti UR, Vijayakumar K. Switched-capacitor-based quadruple-boost nine-level inverter. IEEE Transactions on Power Electronics 2019; 34 (8): 7147-7150.

[12] Khoun Jahan H, Abapour M, Zare K. Switched-capacitor-based single-source cascaded h-bridge multilevel inverter featuring boosting ability. IEEE Transactions on Power Electronics 2019; 34 (2): 1113-1124.

[13] Lee SS. Single-stage switched-capacitor module (s3cm) topology for cascaded multilevel inverter. IEEE Transactions on Power Electronics 2018; 33 (10): 8204-8207.

[14] Liu J, Cheng KWE, Ye Y. A cascaded multilevel inverter based on switched-capacitor for high-frequency ac power distribution system. IEEE Transactions on Power Electronics 2014; 29 (8): 4219-4230.

[15] Ye Y, Cheng KWE, Liu J, Ding K. A step-up switched-capacitor multilevel inverter with self-voltage balancing. IEEE Transactions on Industrial Electronics 2014; 61 (12): 6672-6680.

[16] Ellabban O, Abu-Rub H. Z-source inverter: topology improvements review. IEEE Industrial Electronics Magazine 2016; 10 (1): 6-24.

[17] Siwakoti YP, Peng FZ, Blaabjerg F, Loh PC, Town GE. Impedance-source networks for electric power conversion part i: a topological review. IEEE Transactions on Power Electronics 2015; 30 (2): 699-716.

[18] Tang Y, Fu D, Wang T, Xu Z. Hybrid switched-inductor converters for high step-up conversion. IEEE Transactions on Industrial Electronics 2015; 62 (3): 1480-1490.

[18] Nguyen M, Duong T, Lim Y. Switched-capacitor-based dual-switch high-boost dc–dc converter. IEEE Transactions on Power Electronics 2018; 33 (5): 4181-4189.

[19] Nguyen M, Duong T, Lim Y, Kim Y. Switched-capacitor quasi-switched boost inverters. IEEE Transactions on Industrial Electronics 2018; 65 (6): 5105-5113. 3416LAHOOTI-ESHKEVARI et al./Turk J Elec Eng & Comp Sci

[20] Ajaykumar T, Patne NR. Fault-tolerant switched capacitor–based boost multilevel inverter. International Journal of Circuit Theory and Applications 2019; 47 (10): 1615-1629.

[21] Chang YH, Wu MZ. Switched-capacitor-voltage-multiplier boost dc–ac inverter with adaptive stages. International Journal of Circuit Theory and Applications 2013; 41 (2): 128-149.

[22] Su J, Sun D. Simplified mpcc for four-switch three-phase inverter-fed pmsm. Electronics Letters 2017; 53

(23): 1108-1109. [16] Zeng Z, Zhu C, Jin X, Shi W, Zhao R. Hybrid space vector modulation strategy for torque ripple minimization in three-phase four-switch inverter-fed pmsm drives. IEEE Transactions on Industrial Electronics 2017; 64 (3): 2122-2134.

[24] Metwaly MK. Direct torque and flux control of a four-switch three-phase inverter-fed synchronous reluctance motor drives. Electric Power Components and Systems 2017; 45 (11): 1202-1216.

[25] Kivanc OC, Ozturk SB. Sector determination for SVPWM based four-switch three-phase VSI. Electronics Letters 2017; 53 (5): 343-345.

[26] Zhu C, Zeng Z, Zhao R. Adaptive suppression method for dc-link voltage offset in three-phase four-switch inverterfed pmsm drives. Electronics Letters 2016; 52 (17): 1442-1444.

[27] Zhou W, Sun D. Adaptive pwm for four-switch three-phase inverter. Electronics Letters 2015; 51 (21): 1690-1692.

[28] Liu Y, Ge X, Zhang J, Feng X. General svpwm strategy for three different four-switch three-phase inverters. Electronics Letters 2015; 51 (4): 357-359.

[29] Metwally MK, Azazi HZ. Four-switch three-phase inverter performance fed sensorless speed control induction motor drives using model reference adaptive system. Electric Power Components and Systems 2014; 42 (7): 727-736.

[30] Kashif SAR, Saqib MA. Sensorless control of a permanent magnet synchronous motor using artificial neural network based estimator—an application of the four-switch three-phase inverter. Electric Power Components and Systems 2014; 42 (1): 1-12.